

# Semi-supervised Text-based Person Search

Daming Gao  
Soochow University  
Suzhou, China  
dmgao@stu.suda.edu.cn

Yang Bai  
Soochow University  
Suzhou, China  
ybaibyougert@stu.suda.edu.cn

Min Cao\*  
Soochow University  
Suzhou, China  
mcao@suda.edu.cn

Hao Dou  
Meituan  
Beijing, China  
douhao05@meituan.com

Mang Ye  
Wuhan University  
Wuhan, China  
yemang@whu.edu.cn

Min Zhang  
Soochow University  
Suzhou, China  
minzhang@suda.edu.cn

## ABSTRACT

Text-based person search (TBPS) aims to retrieve images of a specific person from a large image gallery based on a natural language description. Existing methods rely on massive annotated image-text data to achieve satisfactory performance in fully-supervised learning. It poses a significant challenge in practice, as acquiring person images from surveillance videos is relatively easy, while obtaining annotated texts is challenging. The paper undertakes a pioneering initiative to explore TBPS under the semi-supervised setting, where only a limited number of person images are annotated with textual descriptions while the majority of images lack annotations. We present a two-stage basic solution based on generation-then-retrieval for semi-supervised TBPS. The generation stage enriches annotated data by applying an image captioning model to generate pseudo-texts for unannotated images. Later, the retrieval stage performs fully-supervised retrieval learning using the augmented data. Significantly, considering the noise interference of the pseudo-texts on retrieval learning, we propose a noise-robust retrieval framework that enhances the ability of the retrieval model to handle noisy data. The framework integrates two key strategies: Hybrid Patch-Channel Masking (PC-Mask) to refine the model architecture, and Noise-Guided Progressive Training (NP-Train) to enhance the training process. PC-Mask performs masking on the input data at both the patch-level and the channel-level to prevent overfitting noisy supervision. NP-Train introduces a progressive training schedule based on the noise level of pseudo-texts to facilitate noise-robust learning. Extensive experiments on multiple TBPS benchmarks show that the proposed framework achieves promising performance under the semi-supervised setting.

## CCS CONCEPTS

• Computing methodologies → Artificial intelligence; • Information systems → Image search.

## KEYWORDS

text-based person search; semi-supervised learning; noise-robust learning; learning with masking; curriculum learning

## 1 INTRODUCTION

Text-based person search (TBPS) [31, 34] aims at retrieving the target person images from a large image gallery using natural language descriptions, with promising applications in surveillance

\*Corresponding author.

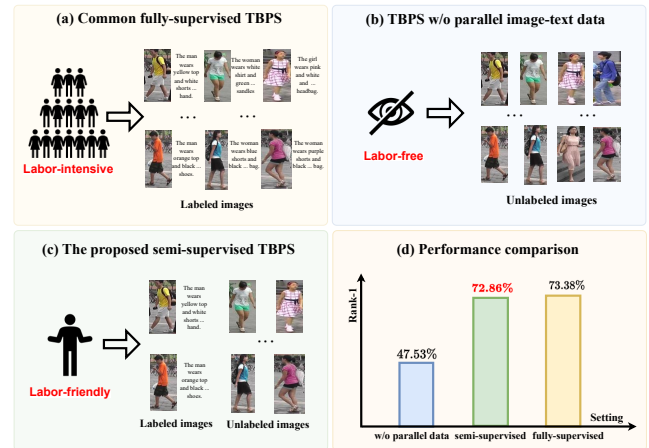





Figure 1: Comparisons with (a) common fully-supervised TBPS, (b) TBPS w/o parallel image-text data and (c) the proposed semi-supervised TBPS, and (d) performance comparison of the methods with above settings (i.e., the method [2] for TBPS w/o parallel image-text data and the method [21] for the fully-supervised TBPS) on CUHK-PEDES [31].

systems. TBPS shares connections with image-based person re-identification [27, 49] and image-text retrieval [6, 7] and yet presents unique challenges. Unlike image-based person re-identification, TBPS utilizes open-form textual queries for more flexible search information, while dealing with cross-modal discrepancies due to modality heterogeneity. Compared to image-text retrieval, TBPS focuses on person domain retrieval, introducing the challenge of smaller inter-class variation and requiring enhanced perception and reasoning over fine-grained information.

To address these challenges, researchers have introduced various TBPS approaches [5, 30, 44, 52], which focus on learning discriminative and modality-invariant feature representations, employing diverse fine-grained cross-modal alignment modules. These efforts have yielded promising performance improvements, and yet come at the cost of requiring a substantial number of image-text pairs for training the model (Fig. 1(a)). This requirement is impractical in real-world scenarios due to the manual annotation typically involved. To address this limitation, few works [2, 24, 53] have explored TBPS without relying on a fully-supervised setting, thus reducing the burden of annotating. Zhao et al. [53] introduced a weakly supervised TBPS method that eliminates the need for identity labeling. Jing et al. [24] developed a domain-adaptive TPBS approach, training

Image	BLIP zero-shot	BLIP finetuned	Human annotated
	Boy running down the street in red and blue sneakers.	He wears a red shirt with white shorts and blue shoes he carries a black backpack.	A man in a red shirt, a pair of blue jean shorts and a pair of blue shoes with white socks.
	A girl crossing the street with her umbrella in hand.	A woman wearing a pink top, a <b>gray and white skirt</b> , brown shoes and a white purse.	A woman with long dark hair is wearing a coral long sleeved blouse, a long skirt and sandals.
	A boy skateboarding down a city street in a yellow shirt.	A man with short black hair wearing yellow shirt and <b>blue jeans</b> carrying a black bag.	He has short black hair and is wearing a bright yellow shirt. He is also wearing denim pants.

**Figure 2: Visualization of human annotated texts and generated pseudo-texts from the vision-language model BLIP [29] under the zero-shot setting and finetuned on 1% labeled data. Pseudo-texts from zero-shot BLIP tend to be coarse-grained while those from finetuned BLIP possess more fine-grained details but may contain inevitable noise. The noise is highlighted in red. More examples are shown in the Appendix.**

a model on a source domain using supervised learning and then applying it to a new target domain. Bai et al. [2] were the pioneers of TBPS without parallel image-text data, removing the need for annotations. The first two works did not completely eliminate the need for annotations in massive image-text pairs, whereas only the last one achieved a complete release of annotations (Fig.1(b)). However, this work yields inadequate retrieval performance due to the complete absence of annotations (Fig.1(d)).

Considering the trade-off between annotation cost and retrieval performance, this paper presents the first attempt at a practical setting: semi-supervised TBPS. In this setting, the model is trained with access to a small number of person image-text pairs and a large collection of person images<sup>1</sup> (Fig.1(c)). While semi-supervised learning has been explored for general image-text retrieval [19, 25], its exploration within the TBPS community remains limited to the best of our knowledge. Developing a semi-supervised TBPS solution is essential to achieve excellent performance with minimal annotation costs. Nevertheless, TBPS poses unique challenges in semi-supervised learning compared to the general image-text retrieval task, primarily due to its specialization in the person domain and the inclined demand for modeling fine-grained information.

For this, we firstly develop a two-stage basic solution based on generation-then-retrieval. In the generation stage, an off-the-shelf image captioning model finetuned on the few labeled data is applied to generate pseudo-textual descriptions for the unlabeled person images, and thus the deficiency of the labeled data can be alleviated by incorporating the pseudo-labeled data. In the retrieval stage, the retrieval model is trained with the combined few labeled data and pseudo-labeled data in a fully-supervised learning manner. Remarkably, the fine-grained characteristic of TBPS brings the risk that the pseudo-texts may not always align well with the person images (BLIP finetuned vs. Human annotated in Fig. 2). This inevitable noise may put the retrieval model at risk of learning misalignment.

<sup>1</sup>In real-world scenarios, obtaining person images from surveillance videos via person detection technologies [4, 50] is relatively straightforward, while acquiring paired textual descriptions often necessitates manual annotation.

To overcome this issue, we propose a noise-robust retrieval framework to enhance the ability of retrieval model to handle noisy labeled data. This framework integrates noise-robust design principles to the model architecture and the training strategy. For the model architecture, we introduce a hybrid patch-channel masking (PC-Mask), combining patch-level and channel-level masking. Patch-level masking randomly masks a portion of the input data in the original semantic space, while channel-level masking randomly masks feature values in the computed representation space. By leveraging their complementary effects, PC-Mask effectively decouples the underlying noisy correspondence in image-text pairs and prevents the retrieval model from overfitting the noisy supervision. For the training strategy, we design a noise-guided progressive training (NP-Train), inspired by curriculum learning [43]. NP-Train schedules the training in a progressive manner. It starts by utilizing more reliable data with less noise and gradually introduces more challenging data with higher noise levels. This strategy ensures that the model is dominated by high-confidence data, alleviating the interference from noisy data. By applying PC-Mask and NP-Train to the retrieval model (e.g., RaSa [1] and IRRRA [21]), we establish a noise-robust retrieval framework, which facilitates the cross-modal representation learning in the presence of noisy training data.

Our contributions can be summarized as follows. (1) We make the first exploration of semi-supervised TBPS, which is a more resource-friendly and realistic scenario than the much-studied fully-supervised TBPS in the current community. A two-stage solution based on generation-then-retrieval is presented to address this novel setting. (2) In order to tackle the noise interference resulting from generated pseudo-labeled data during the training of retrieval model, we propose a noise-robust retrieval framework. It integrates two key strategies: hybrid patch-channel masking for refining the model architecture, and noise-guided progressive training for enhancing the training process. (3) Extensive experiments demonstrate that the proposed framework can achieve promising performance under the semi-supervised setting.

## 2 RELATED WORK

### 2.1 Text-based Person Search

Current TBPS methods [1, 5, 21, 30, 44, 52] can be classified into two categories: cross-modal alignment and pretext task design. The former aligns visual and textual features in a shared embedding space, while the latter designs pretext tasks for learning modality-invariant features. Specifically, for cross-modal alignment, early studies focused on global alignment [52, 54] but later advanced to local alignment [8, 33], such as patch-word or region-phrase correspondences. Also, self-adaptive methods [13, 30] were proposed to learn multi-granularity alignment, and some studies [23, 44] incorporated external technologies like human parsing and pose estimation to aid alignment. For pretext task design, Wu *et al.* [45] designed two color-reasoning sub-tasks to enable models to learn representations; Bai *et al.* [1] formulated the relation and sensitivity-aware learning tasks to address weak cross-modal correspondence; Jiang *et al.* [21] introduced a cross-modal implicit relation reasoning task to enhance the learning of fine-grained representation.

The mentioned methods heavily depend on fully annotated data, which is challenging to obtain in real-world scenarios due to its cost

and time requirements. Several works [2, 24, 53] have begun exploring TBPS in non-supervised settings, aiming to alleviate the burden of annotation from various perspectives. Jing *et al.* [24] addressed the domain-adaptive TPBS, where they adapted the proposed moment alignment model trained on a source domain to a new and different target domain. Zhao *et al.* [53] introduced weakly supervised TBPS, eliminating the need for identity labeling. They employed a mutual training framework to generate and refine pseudo labels. Bai *et al.* [2] pioneered TBPS without parallel image-text data, completely removing the requirement for textual annotations. They explored a fine-grained image captioning strategy to generate pseudo-texts and a confidence-based training scheme to ensure reliable representation learning. However, the domain-adaptive TPBS [24] requires abundant annotated data in the source domain, while weakly supervised TBPS [53] still requires textual annotations for a large number of images, making both approaches impractical due to the expense and time involved in annotation. Although Bai *et al.* [2] eliminated the need for textual annotation, generating pseudo-texts for the task requires additional prior knowledge and intricate rule design. This leads to lower-quality generated texts and limited performance in training retrieval models.

To this end, this paper explores semi-supervised TBPS, aiming to annotate a small amount of data while maximizing the use of readily available resources, specifically person images from surveillance cameras, to achieve satisfactory performance. Both Bai *et al.* [2] and our work adopt the generation-then-retrieval paradigm, where pseudo-labeled data is initially generated and used for retrieval training. However, our work focuses on noise-robust learning with pseudo-labeled data in the retrieval stage, while Bai *et al.* [2] emphasizes the image captioning strategy in the generation stage.

## 2.2 Learning with Noisy Data

The issue of noisy data in cross-modal scenarios has gained increasing attention recently, with a focus on learning robust representations from mismatched multimodal data pairs. Several methods have been proposed to mitigate the negative impact of noisy supervision. For example, Huang *et al.* [20] introduced the NCR framework, which partitions data into clean and noisy subsets based on neural network memorization and rectifies correspondence adaptively. Qin *et al.* [37] developed an evidential learning paradigm that captures noise uncertainty and mitigates its adverse effects with a dynamic hinge loss. Han *et al.* [15] approached the problem from a meta-learning standpoint and proposed a data purification strategy to remove noisy samples. Additionally, Qin *et al.* [36] addressed the noisy correspondence issue in TBPS, employing a confident consensus mechanism to partition noisy samples and introducing triplet alignment loss to reduce the misleading risks in training. The previous studies address the noisy data problem in completely mismatched image-text pairs. However, in our scenario, the pseudo-texts are weakly correlated with the person images, containing partial semantic noise interference. Thus, these existing approaches cannot be directly applied. To achieve robust learning with weakly labeled pseudo-texts, we propose NP-Train, which schedules training based on quantified noise scores, and PC-Mask, which provides additional learning regularization.

## 2.3 Learning with Masking

In natural language processing, masked language modeling (MLM) derived from BERT [9] is a widely used pretraining task, which masks parts of input sentences and trains models to predict the missing content, resulting in pretrained representations with strong generalization capabilities [39, 42, 51]. Similarly, the masked auto-encoder (MAE) [16] applies the concept to computer vision by masking and reconstructing random image patches, leading to generalized representations and superior performance. Inspired by MAE, FLIP [32] leverages masking for vision-language pretraining with expanded scale. The proposed PC-Mask follows a similar paradigm but differs in its purpose. Instead of reconstruction, we utilize masking as a regularization strategy to address the noisy interference from pseudo-labeled training data.

## 2.4 Curriculum Learning

Curriculum learning (CL), introduced by Bengio *et al.* [3], is a training strategy that starts with easy examples and progresses to more difficult ones, resembling human learning curricula. CL is commonly used for denoising by prioritizing high-confidence, less complex data to mitigate the impact of noise [43]. For instance, Jiang *et al.* [22] proposed MentorNet, which applies a data-driven curriculum to focus on potentially correct-labeled data, significantly improving network generalizability on corrupted data. Guo *et al.* [14] designed a curriculum that quantifies noise levels using cluster density measurements, enabling robust training on noisy web images. Inspired by CL for denoising, we propose NP-Train to learn reliable cross-modal relations on noisy data.

## 3 METHODOLOGY

In semi-supervised text-based person search, we are given a labeled dataset  $\mathcal{D}_l = \{I_i, T_i\}_{i=1}^{N_l}$ . Here,  $I_i$  denotes the  $i$ -th image,  $T_i$  is the  $i$ -th textual description paired with  $I_i$ ,  $N_l$  is the total number of image-text pairs. Notably, this number is significantly smaller compared to the fully supervised counterpart. Additionally, we are also provided with an unlabeled dataset of person images  $\mathcal{D}_u = \{I_i\}_{i=1}^{N_u}$ , wherein corresponding text annotations are absent. Building upon the generation-then-retrieval solution, we introduce a noise-robust retrieval framework that aims to achieve promising performance utilizing both labeled data ( $\mathcal{D}_l$ ) and unlabeled data ( $\mathcal{D}_u$ ). Fig. 3 provides an overview of the proposed generation-then-retrieval solution, which incorporates a noise-robust retrieval framework.

In the subsequent sections, we begin by outlining the basic two-stage solution rooted in the generation-then-retrieval course. We then detail the noise-robust retrieval framework, including the proposed hybrid patch-channel masking and noise-guided progressive training. For simplicity, we will use  $I$  and  $T$  to represent an image and a text, respectively, while omitting the symbolic subscripts.

### 3.1 Basic Solution: Generation-Then-Retrieval

To handle the semi-supervised TBPS, we firstly introduce a basic two-stage solution. In the generation stage, we leverage the few labeled data ( $\mathcal{D}_l$ ) to generate pseudo-labels for the unlabeled data ( $\mathcal{D}_u$ ), to enrich the training corpus. In the retrieval stage, a retrieval model is trained, utilizing both the labeled data and the generated pseudo-labeled data in a supervised manner.

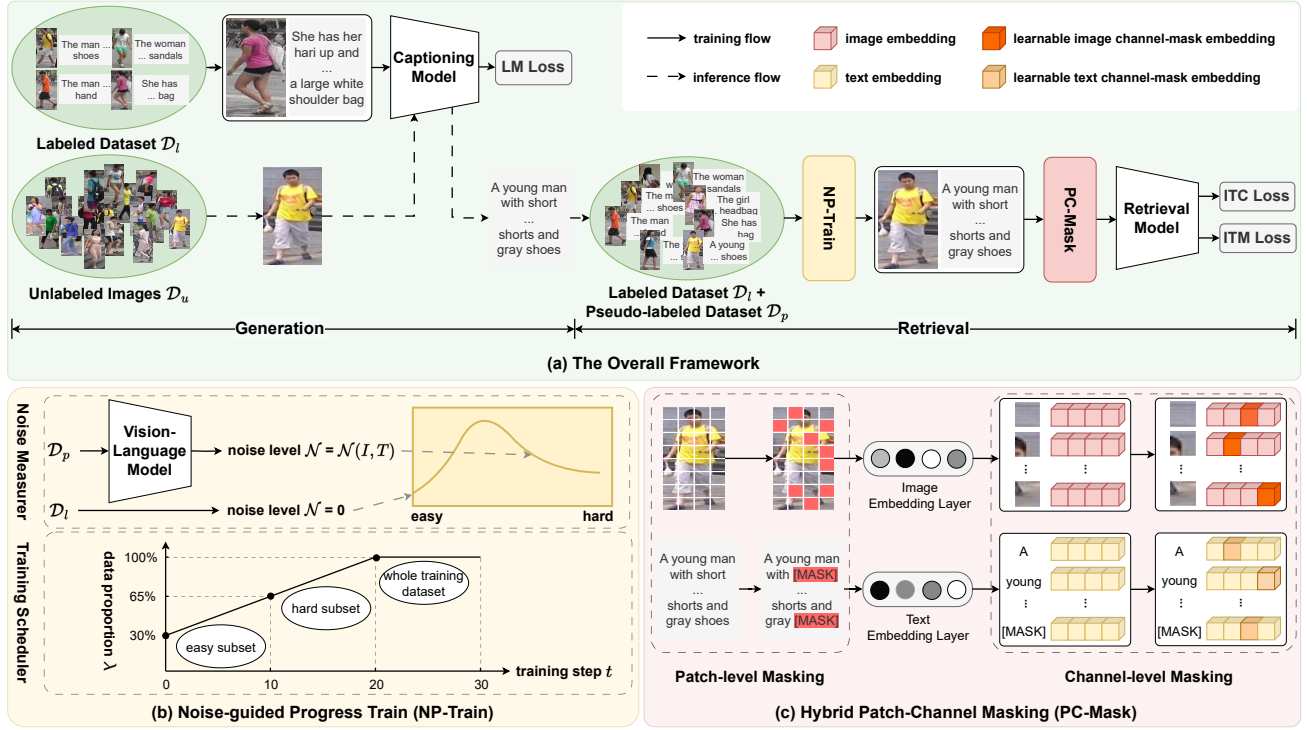


Figure 3: Illustration of the proposed generation-then-retrieval solution along with the noise-robust retrieval framework.

### 3.1.1 Generation.

Generating textual descriptions for person images in dataset  $\mathcal{D}_u$  can be viewed as an image captioning task [46], for which an off-the-shelf image captioning model can be employed. However, it is important to note that current image captioning models [28, 29] are typically trained on generic image-text corpus data, which results in a noticeable gap when dealing with person-specific data. If directly applying such models to person images, the generated texts may lack fine-grained details and fail to capture the subtle information related to the appearance of individuals, as shown in Fig. 2 (BLIP zero-shot vs. Human annotated). Consequently, this can harm the subsequent retrieval stage, which heavily relies on precise cross-modal alignment learning.

Hence, we employ the few labeled data  $\mathcal{D}_l$  to finetune the image captioning model, so that the person-related knowledge and the fine-grained captioning ability of the model can be learned. Specifically, given an image  $I$  and its paired text  $T = \{u_1, u_2, \dots, u_n\}$  from  $\mathcal{D}_l$ , where  $u_i$  is the  $i$ -th token in the text, we minimize the following language modeling loss during finetuning:

$$\mathcal{L}_{lm} = - \sum_{i=1}^n \log P(u_i | I, u_1, u_2, \dots, u_{i-1}; \Theta), \quad (1)$$

where the conditional probability  $P$  is computed using an image captioning model with parameters  $\Theta$ .

After finetuning on the few labeled data, we use the image captioning model to generate pseudo-texts for each unlabeled person image within dataset  $\mathcal{D}_u$ . The resulting collection of pseudo-labeled data is represented as  $\mathcal{D}_p = \{I_i, T_i\}_{i=1}^{N_p}$ , where  $N_p$  is the total number of pseudo-labeled image-text pairs.

### 3.1.2 Retrieval.

We combine the few pre-existing labeled dataset  $\mathcal{D}_l$  with the newly-generated pseudo-labeled dataset  $\mathcal{D}_p$  to create the training set for the retrieval stage. The default retrieval model, BLIP [29], is adopted, and its network architecture, described here, serves as the foundation for the proposed noise-robust retrieval framework. BLIP is an advanced vision-language model with remarkable performance on various vision-language tasks. It has three modules.

**Image Encoder.** Visual transformer [11] is employed as the image encoder. Given an input image  $I$ , we first splits it into a sequence of  $M$  non-overlapping patches,  $p_i \in \mathbb{R}^{h \times w}$  ( $i = 1, \dots, M$ ). Then a linear projection  $\mathbf{L}^v$  operates on the patches and obtain 1D tokens  $v_i \in \mathbb{R}^d$ . It can be formulated as:

$$\mathcal{V} = [v_{cls}, \mathbf{L}^v(p_1), \mathbf{L}^v(p_2), \dots, \mathbf{L}^v(p_M)] + P^v, \quad (2)$$

where  $v_{cls} \in \mathbb{R}^d$  is a learnable classification token and  $P^v \in \mathbb{R}^{(M+1) \times d}$  is the positional embedding.

Next, we send the embedding sequence  $\mathcal{V}$  into the image encoder  $\mathbf{E}^v$  to extract image features  $\mathcal{F}_o \in \mathbb{R}^{(M+1) \times d}$ , which can be formulated as:

$$\mathcal{F}_o = \mathbf{E}^v(\mathcal{V}), \quad (3)$$

wherein  $f_{cls}^v \in \mathbb{R}^d$  represents the global feature of the image  $I$ .

**Text Encoder.** It shares the same architecture with BERT [9]. Given a input text  $T$ , we first tokenizes it into a sequence of  $N$  tokens  $w_i$  ( $i = 1, \dots, N$ ). Then a embedding layer  $\mathbf{L}^t$  is employed to process the tokens and generate 1D embeddings  $t_i \in \mathbb{R}^d$ . This process can be expressed as follows:

$$\mathcal{T} = [t_{cls}, \mathbf{L}^t(w_1), \mathbf{L}^t(w_2), \dots, \mathbf{L}^t(w_N)] + P^t, \quad (4)$$

where  $t_{cls} \in \mathbb{R}^d$  is a learnable embedding and  $P^t \in \mathbb{R}^{(N+1) \times d}$  is the positional embedding of text data.

The embedding sequence  $\mathcal{T}$  is passed via the text encoder  $\mathbf{E}^t$  to extract text features  $\mathcal{F}^t \in \mathbb{R}^{(N+1) \times d}$ . It is formulated as follows:

$$\mathcal{F}^t = \mathbf{E}^t(\mathcal{T}), \quad (5)$$

wherein  $f_{cls}^t \in \mathbb{R}^d$  is the global feature of the text  $T$ .

**Image-grounded Text Encoder.** The objective is to integrate the image and text features, enabling comprehensive interaction between the visual and textual modalities. The encoder enhances the text encoder by incorporating an extra cross-attention layer within each transformer block. Specifically, by utilizing the text embeddings  $\mathcal{T}$  as query and the image features  $\mathcal{F}^v$  as key and value, the encoder  $\mathbf{E}^m$  generates a sequence of multimodal fused features  $\mathcal{F}^m \in \mathbb{R}^{(N+1) \times d}$ , which can be formulated as:

$$\mathcal{F}^m = \mathbf{E}^m(\mathcal{T}, \mathcal{F}^v), \quad (6)$$

wherein  $f_{cls}^m$  is the fused feature of the image  $I$  and the text  $T$ .

**Training Objectives.** Following BLIP, we optimize the retrieval model using the image-text contrastive loss (ITC) and image-text matching loss (ITM). ITC aligns the feature space of the image encoder and text encoder by bringing positive image-text pairs closer and pushing negative pairs apart, and operates on  $f_{cls}^v$  and  $f_{cls}^t$ . ITM aims to learn the multimodal fused feature  $f_{cls}^m$  that captures cross-modal alignment by predicting the positivity (match) or negativity (mismatch) of image-text pairs. Refer to the original paper of BLIP [29] for the formula details.

The overall training objective is defined as:

$$\mathcal{L} = \mathcal{L}_{itc} + \mathcal{L}_{itm}. \quad (7)$$

We train the retrieval model BLIP with Eq. 7 on the training sets  $\mathcal{D}_p$  and  $\mathcal{D}_l$  in a supervised manner.

## 3.2 Hybrid Patch-channel Masking

As the pseudo-texts in  $\mathcal{D}_p$  contain noise that can hinder the retrieval model's ability to learn precise cross-modal alignment, we enhance the above basic solution by integrating Hybrid Patch-channel Masking (PC-Mask) into the retrieval model for alleviating the impact of noise. PC-Mask applies masking at both the patch-level and the channel-level, as introduced in the following section.

### 3.2.1 Patch-level Masking.

This strategy masks parts of the input data in the original semantic space, which is conducted on both the visual and textual modality.

For the visual modality, given the sequence of patches from an input image  $I$ , we randomly mask out a portion of the patches with the masking ratio  $\rho^v$  by simply removing them and the remaining patches are inputted into the network. Hence, Eq. 2 is rewritten as:

$$\mathcal{V}' = [v_{cls}, \mathbf{L}^v(p_1), \mathbf{L}^v(p_2), \dots, \mathbf{L}^v(p_{M'})] + P^v, \quad (8)$$

where  $M' = M(1 - \rho^v)$  is the number of unmasked patches.

In terms of the textual modality, given the sequence of tokens from an input text  $T$ , we randomly sample a subset of the tokens with the masking ratio  $\rho^t$  and replace them with the special [MASK] token. The masked sequence of tokens are passed to the network and thus Eq. 4 is rewritten as:

$$\mathcal{T}' = [t_{cls}, \mathbf{L}^t(w_1), \mathbf{L}^t([\text{MASK}]), \dots, \mathbf{L}^t(w_N)] + P^t, \quad (9)$$

### 3.2.2 Channel-level Masking.

The strategy involves masking the feature channels within the computed representation space and is also employed in both the visual and textual modalities.

For the visual modality, we mask a subset of channel values in the patch embeddings  $\mathcal{V}'$  in Eq. 8. Specifically, we first incorporate a learnable channel-mask embedding  $c^v \in \mathbb{R}^d$  as a prototype. Next, for each embedding  $v_i$  ( $i = 1, 2, \dots, M'$ ) in Eq. 8, we randomly sample a portion of its channel values using the masking ratio  $\beta^v$ . These sampled values are then replaced with the corresponding channel values from  $c^v$ . This process can be represented as:

$$\mathcal{V}'' = [v_{cls}, \mathbf{M}(\mathbf{L}^v(p_1)), \mathbf{M}(\mathbf{L}^v(p_2)), \dots, \mathbf{M}(\mathbf{L}^v(p_{M'}))] + P^v, \quad (10)$$

$$\mathbf{M}(\mathbf{L}^v(p_i)) = \mathbf{L}^v(p_i) \odot b^v + c^v \odot (1 - b^v), \quad i = 1 \dots M' \quad (11)$$

where  $b^v \in \mathbb{R}^d$  is a random binary mask vector (0 with probability  $\beta^v$  and 1 with probability  $1 - \beta^v$ ), and  $\odot$  is the hadamard product.

The sequence of embeddings  $\mathcal{V}''$  is then sent to the image encoder to obtain the final features  $\mathcal{F}_v''$ , as depicted in Eq. 3.

Similar to the operations performed on the visual modality, we apply channel-level masking to the embedding sequence  $\mathcal{T}'$  in Eq. 9 for the textual modality. This masking involves a learnable channel-mask embedding  $c^t \in \mathbb{R}^d$  and the masking ratio  $\beta^t$ . The outputted masked embeddings  $\mathcal{T}''$  are then fed into the text encoder to obtain the final features  $\mathcal{F}_t''$ , as shown in Eq. 5.

Using the masked textual embeddings  $\mathcal{T}''$  and the masked visual features  $\mathcal{F}_v''$ , we generate the multimodal fused features  $\mathcal{F}_m''$  by inputting them into the image-grounded text encoder as described in Eq. 6. During the training process, we optimize the ITC and ITM loss functions using the masked features  $\mathcal{F}_v''$ ,  $\mathcal{F}_t''$ , and  $\mathcal{F}_m''$ . During inference, we apply the retrieval model to the original image and text inputs without masking.

In short, PC-Mask decouples the noisy correspondence across modalities by randomly masking data. This random operation can be considered as a form of data regularization to prevent overfitting during training with noisy data.

## 3.3 Noise-guided Progressive Training

In addition to PC-Mask, we also developed a Noise-Guided Progressive Training strategy (NP-Train) aimed at achieving noise-robust training. Instead of treating all generated pseudo-labeled data equally during training, regardless of their varying levels of noise, NP-Train follows a progression from more reliable data with less noise to more challenging data with higher levels of noise.

In this process, two modules are designed: the *Noise Measurer*, which evaluates the noise level of each pseudo-text, and the *Training Scheduler*, which determines the sequence of data subsets throughout the training process based on the noise level of data. In the following, we elaborate on these two modules.

### 3.3.1 Noise Measurer.

The generated pseudo-texts exhibit varying degrees of noise resulting from errors in the image captioning model. This noise pertains to descriptions semantically inconsistent or unrelated to the corresponding images, impeding the model's ability to learn accurate cross-modal alignment.

In this context, the noise measurer assesses the level of noise in each pseudo-text by considering the cross-modal semantic similarity. When a pseudo-text closely aligns with the depicted image, it indicates the strong alignment of cross-modal semantics, resulting in a lower potential for noise in the pseudo-text. Conversely, if a pseudo-text significantly differs from its corresponding image, it signifies a large semantic gap between the image-text pair, suggesting a higher likelihood of noise in the pseudo-text.

Formally, given a pseudo-text  $T$  and its corresponding image  $I$  from the pseudo-labeled training set  $\mathcal{D}_p$ , the level of noise in  $T$  is defined to have a negative correlation with their cross-modal similarity, as expressed below:

$$N(T) = 1 - \psi(I, T), \quad (12)$$

where  $\psi(I, T)$  denotes the matching score of the pair and is computed by the state-of-the-art vision-language models. These models are typically pretrained on massive image-text data, enabling them to capture the cross-modal semantic relationship accurately. By default, we employ the BLIP [29] to calculate the matching scores. Other variants are also used and compared for a comprehensively analysis of noise measurers in Table 2.

### 3.3.2 Training Scheduler.

Using the proposed noise measurer, we arrange the training image-text pairs in  $\mathcal{D}_l + \mathcal{D}_p$  in ascending order based on their assessed noise levels<sup>2</sup>. We schedule the training process by sequentially using these organized training data to optimize the retrieval model. Specifically, we employ the linear scheduler, which linearly adjusts the training data subset at each epoch. It can be formulated as:

$$\lambda_{\text{linear}}(t) = \min\left(1, \lambda_0 + \frac{1 - \lambda_0}{T_{\text{grow}}} \cdot t\right), \quad (13)$$

where  $\lambda_0$  is the initial ratio of the easiest available samples,  $T_{\text{grow}}$  is the epoch when all training samples are used for the first time and  $t$  is the current training epoch number. The function  $\lambda_{\text{linear}}(t)$  is a linear function that maps the training epoch number to a scalar  $\lambda \in (0, 1]$ . It determines the ratio of the easiest training data available at the  $t$ -th epoch. This function is monotonically non-decreasing, starting at  $\lambda(0) > 0$  and concluding at  $\lambda(T) = 1$ . Referring to the method [43],  $\lambda_0$  is set to 0.3 and  $T_{\text{grow}}$  is set to 15 in our experiments.

## 4 EXPERIMENTS

We conduct experiments on three widely-used TBPS datasets: CUHK-PEDES [31], ICFG-PEDES [10] and RSTPReid [55], and a newly released dataset: UFine6926 [56]. For semi-supervised TBPS, we randomly select a small ratio<sup>3</sup> (1%, 5%, and 20%) of labeled training data consisting of person images and their corresponding textual descriptions from the original benchmark set. The remaining person images, without their accompanying texts, are used as the unlabeled dataset in our experiments. We adopt the Rank-k (R-k for simplicity, k=1, 5, 10) as the main evaluation metric and the mean average precision (mAP) as a complementary metric. *The introduction of each dataset, evaluation metrics and the implementation details of the proposed framework are shown in the Appendix.*

<sup>2</sup>The noise level of manually annotated texts in  $\mathcal{D}_l$  is assigned as zero.

<sup>3</sup>Experiments under higher ratios of labeled data are shown in the Appendix.

## 4.1 Backbones

The proposed solution offers flexibility in selecting image captioning and text-based person retrieval backbones. To verify the scalability of the proposed framework, we employ two backbones for captioning in the generation stage: BLIP [29] and BLIP-2 [28], and three retrieval backbones in the retrieval stage: BLIP [29], RaSa [1] and IRRR [21]. We use BLIP as the default choice for generation and retrieval in the following experiments, whose model architecture has been discussed in Section 3.1. *Further details regarding the other backbones can be found in the Appendix.*

## 4.2 Ablation Study

### 4.2.1 Effectiveness of Each Component.

In this section, we analyze the effectiveness of each key component in the proposed framework, including the basic generation-then-retrieval solution (Basic-GTR), PC-Mask and NP-Train, via a series of ablation studies on three commonly-used datasets with 1% labeled data. The experimental results are shown in Table 1.

**Effectiveness of Basic-GTR.** Compared to the baseline that solely includes a retrieval stage by training the retrieval model on 1% labeled dataset, the proposed Basic-GTR (M1) achieves substantial improvements across all three datasets (e.g., from 54.91% to 61.94% at Rank-1 on CUHK-PEDES). This improvement highlights the effectiveness of Basic-GTR in effectively utilizing unlabeled data for semi-supervised TBPS.

**Effectiveness of PC-Mask.** The experimental comparison between M1 and M4 provides compelling evidence for the efficacy of PC-Mask. Specifically, when incorporating PC-Mask into the Basic-GTR framework, the Rank-1 accuracy is improved by 1.41%, 1.41%, and 1.05% on the three datasets, respectively. These results confirm that PC-Mask serves as an effective regularization technique during the training process, reducing the interference of noise originating from the pseudo-labeled data.

**Effectiveness of NP-Train.** Beyond applying PC-Mask to mitigate the negative impact of noise, we introduce NP-Train to facilitate noise-robust learning from the perspective of the training strategy. The effectiveness of NP-Train is revealed via the experimental results of M5 vs. M1. In particular, when integrating with NP-Train, the performance exhibits significant improvement, with the Rank-1 accuracy increasing by 1.12% on the CUHK-PEDES dataset. These results demonstrate that NP-Train effectively enables the model to learn reliable cross-modal relations in noisy circumstances.

Finally, with the synergy of each component, the proposed framework achieves the promising performance of 63.87%, 46.46% and 56.45% at Rank-1 on three datasets using only 1% labeled data and remaining unlabeled data, beating the baseline by a large margin.

### 4.2.2 Analysis on the PC-Mask.

To investigate the inner mechanism of PC-Mask, we provide experimental analysis on the impact of each component inside PC-Mask, including patch-level masking (P-Mask) and channel-level masking (C-Mask). (1) P-Mask decouples the noisy correspondence by masking in the high-level semantic space. Its effectiveness is demonstrated through the experimental results of M2 vs. M1 in Table 1. Integrating P-Mask into the Basic-GTR framework alone leads to significant improvements. (2) C-Mask exerts the masking on the low-level representation space. As shown in the experiments of M3

**Table 1: Ablation studies on each component of the proposed framework on the widely-used datasets with 1% labeled data.**

Methods	Components				CUHK-PEDES		ICFG-PEDES		RSTPReid	
	Basic-GTR	PC-Mask		NP-Train	R-1	mAP	R-1	mAP	R-1	mAP
		P-Mask	C-Mask							
Baseline	-	-	-	-	54.91	47.61	37.14	16.70	52.60	37.78
M1	✓	-	-	-	61.94	55.59	44.30	25.12	55.50	42.40
M2	✓	✓	-	-	63.01	56.64	45.63	26.29	55.40	43.43
M3	✓	-	✓	-	62.48	56.02	45.33	25.46	56.15	43.79
M4	✓	✓	✓	-	63.35	57.06	45.71	26.32	<b>56.55</b>	43.57
M5	✓	-	-	✓	63.06	56.38	46.14	26.64	55.20	42.97
Ours	✓	✓	✓	✓	<b>63.87</b>	<b>57.18</b>	<b>46.46</b>	<b>26.90</b>	56.45	<b>44.45</b>

**Table 2: Comparison with different noise measurers on CUHK-PEDES with 1% labeled data. The default setting is marked in bold.**

Methods	R-1	R-5	R-10	mAP
Random sampling	62.98	81.64	87.43	56.10
Sentence length	61.61	80.72	86.58	55.25
CLIPScore	62.35	81.09	87.33	56.17
<b>BLIPscore</b>	<b>63.87</b>	<b>82.20</b>	<b>87.70</b>	<b>57.18</b>

vs. M1, merely adding C-Mask brings consistent improvements at the Rank-1 accuracy on the three datasets by 0.54%, 1.03%, 0.65%, respectively, demonstrating its effectiveness in noise suppression. (3) When combining the two masking strategies together, the performance gains further improvement (M4 vs. M2/M3), which verifies their underlying complementary nature.

#### 4.2.3 Analysis on the NP-Train.

To further study the effect of Noise-guided Progressive Training (NP-Train), we conduct ablation studies on the two key components of NP-Train, namely noise measurer and training scheduler.

**Comparisons with different noise measurers.** In NP-Train, the noise measurer is critical in deciding the training curriculum. To investigate the effect of our proposed noise measurer, we compare it with different variants, as shown in Table 2. First, we evaluate the performance using *Random sampling*, where the samples are randomly scheduled without considering noise assessment. Second, we conduct experiments using a mono-modal noise measurer called *Sentence length*, which determines the noise criterion based solely on the number of words in a text, following the method [35]. In addition, we compare two noise measurers based on cross-modal semantic similarity: *CLIPScore* [17] and *BLIPscore*. *CLIPScore* calculates image-text compatibility based on the pretrained CLIP model [38]. On the other hand, *BLIPscore* measures cross-modal similarity using our finetuned backbone model, BLIP, trained on a combination of limited labeled data and pseudo-labeled data. From Table 2, we can observe that: (1) Compared with *Random sampling*, our utilization of *BLIPscore* leads to significant improvements at Rank-1 and mAP by 0.89% and 1.08%, respectively. This outcome serves as evidence showcasing the effectiveness of our proposed noise measurer in establishing a meaningful learning curriculum. (2) Generally, the application of noise measurers based on cross-modal semantic similarity (last two rows in Table 2) yields better performance compared to the usage of the mono-modal noise measurer, *Sentence length*.

**Table 3: Comparison with different training schedulers on CUHK-PEDES with 1% labeled data.**

Methods	R-1	R-5	R-10	mAP
Baby step	63.69	82.10	87.82	57.32
Root-2	62.98	81.76	87.49	56.80
<b>Linear</b>	<b>63.87</b>	<b>82.20</b>	<b>87.70</b>	<b>57.18</b>

This observation verifies that the noise presented in pseudo-text primarily manifests at the semantic level. Consequently, measuring noise based on cross-modal consistency proves to be more adequate and superior in capturing and quantifying such noise. (3) Compared with *CLIPScore*, *BLIPscore* shows better performance (e.g. 1.52% improvement at Rank-1), which demonstrates that vision-language models pretrained on the generic domain are inadequate in accurately measuring fine-grained semantic similarity.

**Comparisons with different training schedulers.** Based on the sorted data from the noise measurer, training scheduler further decides the sequence of training data subsets throughout the training process. To investigate the influence of applying different scheduling strategies, we experiment with another two popular training schedulers including *Baby step* [3, 41] and *Root-2* [35]. In the *Baby step* scheduler, the sorted training data is initially divided into buckets. Subsequently, the data is incrementally added bucket by bucket, with an increasing noise amount, after a fixed number of epochs. In contrast to our *Linear* scheduler, which adjusts the training data at each epoch, *Baby step* operates as a discrete scheduler, performing scheduling after a fixed number of epochs. Similar to *Linear*, *Root-2* is also a kind of continuous scheduler which arranges the number of training data at each epoch following a root function. The experimental result is shown in Table 3. (1) *Linear* performs slightly better in terms of Rank-1 accuracy than *Baby step*. We conjecture that this could be attributed to the fact that *Linear* follows a gentler and smoother way in scheduling the training data compared to *Baby step*, which might be advantageous for the optimization process. (2) *Linear* surpasses *Root-2* by a significant margin, with a substantial improvement of 0.89% at Rank-1. We propose that this discrepancy stems from the fact that *Root-2* allocates more training time to data with a higher level of noise compared to *Linear*. Consequently, this allocation may inadvertently amplify the impact of noise interference during the optimization process.

**Table 4: Comparison with SOTA methods on CUHK-PEDES. “Labeled” refers to the amount of labeled training data.**

Labeled	Methods	References	R-1	R-5	R-10	mAP
100%	ViTAA [44]	ECCV 2020	55.97	75.84	83.52	51.60
	DSSL [55]	ACMMM-2021	59.98	80.41	87.56	-
	SAF [30]	ICASSP-2022	64.13	82.62	88.40	58.61
	LGUR [40]	ACMMM-2022	65.25	83.12	89.00	-
	CFine [47]	TIP-2023	69.57	85.93	91.15	-
	IRRA [21]	CVPR-2023	73.38	89.93	93.71	66.13
	TBPS-CLIP [5]	AAAI-2024	73.54	88.19	92.35	65.38
	APTm [48]	ACMMM-2023	76.53	90.04	94.15	66.91
	RaSa [1]	IJCAI-2023	76.51	90.29	94.25	69.38
	GTR [2]	ACMMM-2023	47.53	68.23	75.91	42.91
20%	IRRA [21]	CVPR-2023	61.73	82.31	88.78	54.86
	RaSa [1]	IJCAI-2023	67.22	85.17	90.30	58.83
	Ours	-	72.86	88.08	92.30	65.25
5%	IRRA [21]	CVPR-2023	46.91	69.61	78.25	41.63
	RaSa [1]	IJCAI-2023	56.92	77.63	84.37	49.08
	Ours	-	68.76	85.15	90.56	61.82
1%	IRRA [21]	CVPR-2023	36.52	59.67	69.53	33.46
	RaSa [1]	IJCAI-2023	47.45	67.38	74.69	39.13
	Ours	-	63.87	82.20	87.70	57.18

### 4.3 Comparison with the State-of-the-Arts

We present the comparison results on CUHK-PEDES, ICFG-PEDES, and RSTPreid in Tables 4-6. *The comparison on the recently released dataset UFine6926 is provided in the Appendix.*

Since this paper is the first in semi-supervised TBPS, there are no published works with the same setting that can be fairly compared with the proposed framework. We thus firstly compare the proposed framework with current published methods, which are usually under fully-supervised learning, to indirectly assess its performance. Compared with the methods under the fully-supervised setting (100% Labeled), the proposed framework (20%, 5% or 1% Labeled) exhibits an expected performance gap due to the limited amount of labeled data. However, it still achieves promising results. With only 20% labeled data, the proposed framework achieves competitive results with IRRA, such as 72.86% vs. 73.38% in terms of R-1 on CUHK-PEDES. Notably, it even surpasses the strong method RaSa on RSTPreid, e.g., 67.10% vs. 66.90%. Moreover, the cost savings associated with labeling expenses provided by the proposed framework make it more advantageous for practical applications.

Next, we compare with the unsupervised method GTR (completely abandoning annotations, 0% Labeled) to verify the advantage of the proposed framework in terms of the trade-off between annotation cost and performance. Compared to GTR, the proposed framework demonstrates a significant performance advantage, with respective increases of 16.34%, 18.21%, and 10.85% at Rank-1 on the three datasets using only 1% labeled data.

Finally, we directly assess the performance of the proposed framework by comparing it with two state-of-the-art methods, IRRA and RaSa, under the same settings<sup>4</sup>. As observed, the proposed framework outperforms IRRA and RaSa by a large margin across all labeled ratios. Particularly in the most realistic and challenging scenario where only 1% labeled data is available, the proposed framework surpasses IRRA and RaSa by 27.35% and 16.42% at R-1 on CUHK-PEDES, clearly highlighting the unique advantages of the proposed framework.

<sup>4</sup>The results of IRRA and RaSa under the semi-supervised learning setting are obtained by running their published codes with the limited amount of labeled data.

**Table 5: Comparison with SOTA methods on ICFG-PEDES.**

Labeled	Methods	References	R-1	R-5	R-10	mAP
100%	Dual Path [54]	TOMM-2020	38.99	59.44	68.41	-
	LGUR [40]	ACMMM-2022	57.42	74.97	81.45	-
	CFine [47]	TIP-2023	60.83	76.55	82.42	-
	IRRA [21]	CVPR-2023	63.46	80.25	85.82	38.06
	TBPS-CLIP [5]	AAAI-2024	65.05	80.34	85.47	39.83
	RaSa [1]	IJCAI-2023	65.28	80.40	85.12	41.29
	APTm [48]	ACMMM-2023	68.51	82.99	87.56	41.22
0%	GTR [2]	ACMMM-2023	28.25	45.21	53.51	13.82
20%	IRRA [21]	CVPR-2023	50.32	70.34	77.83	27.83
	RaSa [1]	IJCAI-2023	54.55	71.51	77.34	27.99
	Ours	-	61.65	77.06	82.66	38.53
5%	IRRA [21]	CVPR-2023	35.61	56.95	66.00	19.04
	RaSa [1]	IJCAI-2023	40.88	58.36	65.42	15.86
	Ours	-	55.96	72.12	78.31	34.12
1%	IRRA [21]	CVPR-2023	22.72	41.12	50.28	11.79
	RaSa [1]	IJCAI-2023	30.28	47.64	55.11	9.80
	Ours	-	46.46	64.34	71.60	26.90

**Table 6: Comparison with SOTA methods on RSTPreid.**

Labeled	Methods	References	R-1	R-5	R-10	mAP
100%	DSSL [55]	ACMMM-2021	39.05	62.60	73.95	-
	SSAN [10]	Arxiv-2021	43.50	67.80	77.15	-
	CFine [47]	TIP-2023	50.55	72.50	81.60	-
	IRRA [21]	CVPR-2023	60.20	81.30	88.20	47.17
	TBPS-CLIP [5]	AAAI-2024	61.95	83.55	88.75	48.26
	RaSa [1]	IJCAI-2023	66.90	86.50	91.35	52.31
	APTm [48]	ACMMM-2023	67.50	85.70	91.45	52.56
0%	GTR [2]	ACMMM-2023	45.60	70.35	79.95	33.30
20%	IRRA [21]	CVPR-2023	50.85	74.60	84.70	39.19
	RaSa [1]	IJCAI-2023	58.80	80.90	87.75	44.66
	Ours	-	67.10	85.85	92.00	52.84
5%	IRRA [21]	CVPR-2023	53.45	77.05	86.40	40.18
	RaSa [1]	IJCAI-2023	59.35	80.65	88.00	44.22
	Ours	-	65.60	84.75	90.75	52.29
1%	IRRA [21]	CVPR-2023	32.25	58.85	70.10	26.31
	RaSa [1]	IJCAI-2023	46.35	69.90	78.55	32.58
	Ours	-	56.45	78.95	87.05	44.45

### 4.4 Extended Experiments and Visualization

We carry out extended experiments to validate the scalability of the proposed solution using various backbones and evaluate the generalizability of the noise-robust retrieval framework across different ratios of labeled data. Besides, we also conduct parameter analysis on different masking ratio parameters to investigate the mechanism of our framework. The experimental results can be found in the *Appendix*. For qualitative analysis, we provide retrieval visualization in the *Appendix*, vividly demonstrating the outstanding retrieval capability of the proposed framework.

## 5 CONCLUSION

In this paper, we explore the practical setting of semi-supervised TBPS. We propose a two-stage basic solution based on generation-then-retrieval. Firstly, we address the lack of annotations by generating pseudo-labeled samples. Then, we train a retrieval model in a supervised manner. To handle the noise interference from pseudo-labeled samples during retrieval training, we introduce a noise-robust retrieval framework. This framework consists of two key strategies: Hybrid Patch-Channel Masking (PC-Mask) and Noise-Guided Progressive Training (NP-Train). PC-Mask decouples noisy cross-modal correspondence by masking input data at the



patch-level and channel-level to prevent overfitting to noisy supervision. NP-Train enables noise-robust learning by scheduling training progressively based on the noise level of pseudo-labeled samples. Through extensive experiments on multiple TBPS benchmarks, we demonstrate the effectiveness and superiority of our proposed framework in the semi-supervised setting.

## REFERENCES

- [1] Yang Bai, Min Cao, Daming Gao, Ziqiang Cao, Chen Chen, Zhenfeng Fan, Liqiang Nie, and Min Zhang. 2023. RaSa: Relation and Sensitivity Aware Representation Learning for Text-based Person Search. In *Proceedings of the Thirty-Second International Joint Conference on Artificial Intelligence, IJCAI-23*, Edith Elkind (Ed.), International Joint Conferences on Artificial Intelligence Organization, 555–563. <https://doi.org/10.24963/ijcai.2023/62> Main Track.
- [2] Yang Bai, Jingyao Wang, Min Cao, Chen Chen, Ziqiang Cao, Liqiang Nie, and Min Zhang. 2023. Text-based Person Search without Parallel Image-Text Data. In *Proceedings of the 31st ACM International Conference on Multimedia* (, Ottawa ON, Canada,) (MM '23). Association for Computing Machinery, New York, NY, USA, 757–767. <https://doi.org/10.1145/3581783.3612285>
- [3] Yoshua Bengio, Jérôme Louradour, Ronan Collobert, and Jason Weston. 2009. Curriculum learning (ICML '09). Association for Computing Machinery, New York, NY, USA, 41–48. <https://doi.org/10.1145/1553374.1553380>
- [4] Markus Braun, Sebastian Krebs, Fabian Flohr, and Dariu M Gavrilă. 2019. Eucrocity persons: A novel benchmark for person detection in traffic scenes. *IEEE transactions on pattern analysis and machine intelligence* 41, 8 (2019), 1844–1861.
- [5] Min Cao, Yang Bai, Ziyin Zeng, Mang Ye, and Min Zhang. 2023. An Empirical Study of CLIP for Text-based Person Search. *arXiv preprint arXiv:2308.10045* (2023).
- [6] Min Cao, Shiping Li, Juntao Li, Liqiang Nie, and Min Zhang. 2022. Image-text Retrieval: A Survey on Recent Research and Development. In *Proceedings of the Thirty-First International Joint Conference on Artificial Intelligence, IJCAI-22*, Lud De Raedt (Ed.), International Joint Conferences on Artificial Intelligence Organization, 5410–5417. <https://doi.org/10.24963/ijcai.2022/759> Survey Track.
- [7] Jiacheng Chen, Hexiang Hu, Hao Wu, Yuning Jiang, and Changhu Wang. 2021. Learning the best pooling strategy for visual semantic embedding. In *Proceedings of the IEEE/CVF conference on computer vision and pattern recognition*. 15789–15798.
- [8] Yuhao Chen, Guoqing Zhang, Yujiang Lu, Zhenxing Wang, and Yuhui Zheng. 2022. TIPCB: A simple but effective part-based convolutional baseline for text-based person search. *Neurocomputing* 494 (2022), 171–181.
- [9] Jacob Devlin, Ming-Wei Chang, Kenton Lee, and Kristina Toutanova. 2018. Bert: Pre-training of deep bidirectional transformers for language understanding. *arXiv preprint arXiv:1810.04805* (2018).
- [10] Zefeng Ding, Changxing Ding, Zhiyin Shao, and Dacheng Tao. 2021. Semantically self-aligned network for text-to-image part-aware person re-identification. *arXiv preprint arXiv:2107.12666* (2021).
- [11] Alexey Dosovitskiy, Lucas Beyer, Alexander Kolesnikov, Dirk Weissenborn, Xiuhua Zhai, Thomas Unterthiner, Mostafa Dehghani, Matthias Minderer, Georg Heigold, Sylvain Gelly, et al. 2020. An image is worth 16x16 words: Transformers for image recognition at scale. *arXiv preprint arXiv:2010.11929* (2020).
- [12] Markus Freitag and Yaser Al-Onaizan. 2017. Beam Search Strategies for Neural Machine Translation. In *Proceedings of the First Workshop on Neural Machine Translation*, Thang Luong, Alexandra Birch, Graham Neubig, and Andrew Finch (Eds.), Association for Computational Linguistics, Vancouver, 56–60. <https://doi.org/10.18653/v1/W17-3207>
- [13] Chenyang Gao, Guanyu Cai, Xinyang Jiang, Feng Zheng, Jun Zhang, Yifei Gong, Pai Peng, Xiaowei Guo, and Xing Sun. 2021. Contextual non-local alignment over full-scale representation for text-based person search. *arXiv preprint arXiv:2101.03036* (2021).
- [14] Sheng Guo, Weilin Huang, Haozhi Zhang, Chenfan Zhuang, Dengke Dong, Matthew R. Scott, and Dinglong Huang. 2018. CurriculumNet: Weakly Supervised Learning from Large-Scale Web Images. In *Proceedings of the European Conference on Computer Vision (ECCV)*.
- [15] Haochen Han, Kaiyao Miao, Qinghua Zheng, and Minnan Luo. 2023. Noisy correspondence learning with meta similarity correction. In *Proceedings of the IEEE/CVF Conference on Computer Vision and Pattern Recognition*. 7517–7526.
- [16] Kaiming He, Xinlei Chen, Saining Xie, Yanghao Li, Piotr Dollár, and Ross Girshick. 2022. Masked autoencoders are scalable vision learners. In *Proceedings of the IEEE/CVF conference on computer vision and pattern recognition*. 16000–16009.
- [17] Jack Hessel, Ari Holtzman, Maxwell Forbes, Ronan Le Bras, and Yejin Choi. 2021. CLIPScore: A Reference-free Evaluation Metric for Image Captioning. In *Proceedings of the 2021 Conference on Empirical Methods in Natural Language Processing*, Marie-Francine Moens, Xuanjing Huang, Lucia Specia, and Scott Wen-tau Yih (Eds.), Association for Computational Linguistics, Online and Punta Cana, Dominican Republic, 7514–7528. <https://doi.org/10.1145/3503161.3547922>
- [18] Ari Holtzman, Jan Buys, Li Du, Maxwell Forbes, and Yejin Choi. 2020. The Curious Case of Neural Text Degeneration. In *International Conference on Learning Representations*. <https://openreview.net/forum?id=rygGQyrFvH>
- [19] Yingying Huang, Bingliang Hu, Yipeng Zhang, Chi Gao, and Quan Wang. 2024. A semi-supervised cross-modal memory bank for cross-modal retrieval. *Neuro-computing* (2024), 127430.
- [20] Zhenyu Huang, Guocheng Niu, Xiao Liu, Wenbiao Ding, Xinyan Xiao, Hua Wu, and Xi Peng. 2021. Learning with Noisy Correspondence for Cross-modal Matching. In *Advances in Neural Information Processing Systems*, M. Ranzato, A. Beygelzimer, Y. Dauphin, P.S. Liang, and J. Wortman Vaughan (Eds.), Vol. 34. Curran Associates, Inc., 29406–29419. [https://proceedings.neurips.cc/paper\\_files/paper/2021/file/f5e62af885293cf4d511ceef31e61c80-Paper.pdf](https://proceedings.neurips.cc/paper_files/paper/2021/file/f5e62af885293cf4d511ceef31e61c80-Paper.pdf)
- [21] Ding Jiang and Mang Ye. 2023. Cross-Modal Implicit Relation Reasoning and Aligning for Text-to-Image Person Retrieval. In *IEEE International Conference on Computer Vision and Pattern Recognition (CVPR)*.
- [22] Lu Jiang, Zhengyuan Zhou, Thomas Leung, Li-Jia Li, and Li Fei-Fei. 2018. MentorNet: Learning Data-Driven Curriculum for Very Deep Neural Networks on Corrupted Labels. In *Proceedings of the 35th International Conference on Machine Learning (Proceedings of Machine Learning Research, Vol. 80)*, Jennifer Dy and Andreas Krause (Eds.). PMLR, 2304–2313. <https://proceedings.mlr.press/v80/jiang18c.html>
- [23] Ya Jing, Chenyang Si, Junbo Wang, Wei Wang, Liang Wang, and Tieniu Tan. 2020. Pose-guided multi-granularity attention network for text-based person search. In *Proceedings of the AAAI Conference on Artificial Intelligence*, Vol. 34. 11189–11196.
- [24] Ya Jing, Wei Wang, Liang Wang, and Tieniu Tan. 2020. Cross-modal cross-domain moment alignment network for person search. In *Proceedings of the IEEE/CVF Conference on Computer Vision and Pattern Recognition*. 10678–10686.
- [25] Peipei Kang, Zehang Lin, Zhenguo Yang, Xiaozhao Fang, Alexander M Bronstein, Qing Li, and Wenyin Liu. 2022. Intra-class low-rank regularization for supervised and semi-supervised cross-modal retrieval. *Applied Intelligence* 52, 1 (2022), 33–54.
- [26] Diederik Kingma and Jimmy Ba. 2015. Adam: A Method for Stochastic Optimization. In *International Conference on Learning Representations (ICLR)*. San Diego, CA, USA.
- [27] Qingming Leng, Mang Ye, and Qi Tian. 2019. A survey of open-world person re-identification. *IEEE Transactions on Circuits and Systems for Video Technology* 30, 4 (2019), 1092–1108.
- [28] Junnan Li, Dongxu Li, Silvio Savarese, and Steven Hoi. 2023. BLIP-2: bootstrapping language-image pre-training with frozen image encoders and large language models. In *Proceedings of the 40th International Conference on Machine Learning (Honolulu, Hawaii, USA) (ICML '23)*. JMLR.org, Article 814, 13 pages.
- [29] Junnan Li, Dongxu Li, Caiming Xiong, and Steven Hoi. 2022. Blip: Bootstrapping language-image pre-training for unified vision-language understanding and generation. In *International Conference on Machine Learning*. PMLR, 12888–12900.
- [30] Shiping Li, Min Cao, and Min Zhang. 2022. Learning semantic-aligned feature representation for text-based person search. In *ICASSP 2022-2022 IEEE International Conference on Acoustics, Speech and Signal Processing (ICASSP)*. IEEE, 2724–2728.
- [31] Shuang Li, Tong Xiao, Hongsheng Li, Bolei Zhou, Dayu Yue, and Xiaogang Wang. 2017. Person search with natural language description. In *Proceedings of the IEEE conference on computer vision and pattern recognition*. 1970–1979.
- [32] Yanghao Li, Haoqi Fan, Ronghang Hu, Christoph Feichtenhofer, and Kaiming He. 2023. Scaling Language-Image Pre-Training via Masking. In *Proceedings of the IEEE/CVF Conference on Computer Vision and Pattern Recognition (CVPR)*. 23390–23400.
- [33] Kai Niu, Yan Huang, Wanli Ouyang, and Liang Wang. 2020. Improving description-based person re-identification by multi-granularity image-text alignments. *IEEE Transactions on Image Processing* 29 (2020), 5542–5556.
- [34] Kai Niu, Yanyi Liu, Yuzhou Long, Yan Huang, Liang Wang, and Yanning Zhang. 2024. An Overview of Text-based Person Search: Recent Advances and Future Directions. *IEEE Transactions on Circuits and Systems for Video Technology* (2024).
- [35] Emmanouil Antonios Platanios, Otilia Stretcu, Graham Neubig, Barnabas Poczos, and Tom Mitchell. 2019. Competence-based Curriculum Learning for Neural Machine Translation. In *Proceedings of the 2019 Conference of the North American Chapter of the Association for Computational Linguistics: Human Language Technologies, Volume 1 (Long and Short Papers)*, Jill Burstein, Christy Doran, and Thamar Solorio (Eds.), Association for Computational Linguistics, Minneapolis, Minnesota, 1162–1172. <https://doi.org/10.18653/v1/N19-1119>
- [36] Yang Qin, Yingke Chen, Dezhong Peng, Xi Peng, Joey Tianyi Zhou, and Peng Hu. 2023. Noisy-Correspondence Learning for Text-to-Image Person Re-identification. *arXiv preprint arXiv:2308.09911* (2023).
- [37] Yang Qin, Dezhong Peng, Xi Peng, Xu Wang, and Peng Hu. 2022. Deep Evidential Learning with Noisy Correspondence for Cross-modal Retrieval. In *Proceedings of the 30th ACM International Conference on Multimedia (<conf-loc>, <city>Lisboa</city>, <country>Portugal</country>, </conf-loc>)* (MM '22). Association for Computing Machinery, New York, NY, USA, 4948–4956. <https://doi.org/10.1145/3503161.3547922>

- [38] Alec Radford, Jong Wook Kim, Chris Hallacy, Aditya Ramesh, Gabriel Goh, Sandhini Agarwal, Girish Sastry, Amanda Askell, Pamela Mishkin, Jack Clark, et al. 2021. Learning transferable visual models from natural language supervision. In *International conference on machine learning*. PMLR, 8748–8763.
- [39] Pranav Rajpurkar, Jian Zhang, Konstantin Lopyrev, and Percy Liang. 2016. SQuAD: 100,000+ Questions for Machine Comprehension of Text. In *Proceedings of the 2016 Conference on Empirical Methods in Natural Language Processing*, Jian Su, Kevin Duh, and Xavier Carreras (Eds.). Association for Computational Linguistics, Austin, Texas, 2383–2392. <https://doi.org/10.18653/v1/D16-1264>
- [40] Zhiyin Shao, Xinyu Zhang, Meng Fang, Zhifeng Lin, Jian Wang, and Changxing Ding. 2022. Learning Granularity-Unified Representations for Text-to-Image Person Re-identification. In *Proceedings of the 30th ACM International Conference on Multimedia*. 5566–5574.
- [41] Valentin I. Spitzkovsky, Hiyam Alshawi, and Daniel Jurafsky. 2010. From baby steps to Leapfrog: how “Less is More” in unsupervised dependency parsing. In *Human Language Technologies: The 2010 Annual Conference of the North American Chapter of the Association for Computational Linguistics* (Los Angeles, California) (HLT ’10). Association for Computational Linguistics, USA, 751–759.
- [42] Alex Wang, Amanpreet Singh, Julian Michael, Felix Hill, Omer Levy, and Samuel Bowman. 2018. GLUE: A Multi-Task Benchmark and Analysis Platform for Natural Language Understanding. In *Proceedings of the 2018 EMNLP Workshop BlackboxNLP: Analyzing and Interpreting Neural Networks for NLP*, Tal Linzen, Grzegorz Chrupala, and Afra Alishahi (Eds.). Association for Computational Linguistics, Brussels, Belgium, 353–355. <https://doi.org/10.18653/v1/W18-5446>
- [43] Xin Wang, Yudong Chen, and Wenwu Zhu. 2022. A Survey on Curriculum Learning. *IEEE Transactions on Pattern Analysis and Machine Intelligence* 44, 9 (2022), 4555–4576. <https://doi.org/10.1109/TPAMI.2021.3069908>
- [44] Zhe Wang, Zhiyuan Fang, Jun Wang, and Yezhou Yang. 2020. Vitaa: Visual-textual attributes alignment in person search by natural language. In *Computer Vision—ECCV 2020: 16th European Conference, Glasgow, UK, August 23–28, 2020, Proceedings, Part XII 16*. Springer, 402–420.
- [45] Yushuang Wu, Zizheng Yan, Xiaoguang Han, Guanbin Li, Changqing Zou, and Shuguang Cui. 2021. LapsCore: language-guided person search via color reasoning. In *Proceedings of the IEEE/CVF International Conference on Computer Vision*. 1624–1633.
- [46] Kelvin Xu, Jimmy Ba, Ryan Kiros, Kyunghyun Cho, Aaron Courville, Ruslan Salakhudinov, Rich Zemel, and Yoshua Bengio. 2015. Show, Attend and Tell: Neural Image Caption Generation with Visual Attention. In *Proceedings of the 32nd International Conference on Machine Learning (Proceedings of Machine Learning Research, Vol. 37)*, Francis Bach and David Blei (Eds.). PMLR, Lille, France, 2048–2057. <https://proceedings.mlr.press/v37/xuc15.html>
- [47] Shuanglin Yan, Neng Dong, Liyan Zhang, and Jinhui Tang. 2023. CLIP-Driven Fine-Grained Text-Image Person Re-Identification. *IEEE Transactions on Image Processing* 32 (2023), 6032–6046. <https://doi.org/10.1109/TIP.2023.3327924>
- [48] Shuyi Yang, Yinan Zhou, Zhedong Zheng, Yaxiong Wang, Li Zhu, and Yujiao Wu. 2023. Towards Unified Text-Based Person Retrieval: A Large-Scale Multi-Attribute and Language Search Benchmark. In *Proceedings of the 31st ACM International Conference on Multimedia (<conf-loc>, <city>Ottawa ON</city>, <country>Canada</country>, </conf-loc>)* (MM ’23). Association for Computing Machinery, New York, NY, USA, 4492–4501. <https://doi.org/10.1145/3581783.3611709>
- [49] Mang Ye, Jianbing Shen, Gaojie Lin, Tao Xiang, Ling Shao, and Steven CH Hoi. 2021. Deep learning for person re-identification: A survey and outlook. *IEEE transactions on pattern analysis and machine intelligence* 44, 6 (2021), 2872–2893.
- [50] Xuehui Yu, Yuqi Gong, Nan Jiang, Qixiang Ye, and Zhenjun Han. 2020. Scale match for tiny person detection. In *Proceedings of the IEEE/CVF winter conference on applications of computer vision*. 1257–1265.
- [51] Rowan Zellers, Yonatan Bisk, Roy Schwartz, and Yejin Choi. 2018. SWAG: A Large-Scale Adversarial Dataset for Grounded Commonsense Inference. In *Proceedings of the 2018 Conference on Empirical Methods in Natural Language Processing*, Ellen Riloff, David Chiang, Julia Hockenmaier, and Jun’ichi Tsujii (Eds.). Association for Computational Linguistics, Brussels, Belgium, 93–104. <https://doi.org/10.18653/v1/D18-1009>
- [52] Ying Zhang and Huchuan Lu. 2018. Deep cross-modal projection learning for image-text matching. In *Proceedings of the European conference on computer vision (ECCV)*. 686–701.
- [53] Shizhen Zhao, Changxin Gao, Yuanjie Shao, Wei-Shi Zheng, and Nong Sang. 2021. Weakly supervised text-based person re-identification. In *Proceedings of the IEEE/CVF International Conference on Computer Vision*. 11395–11404.
- [54] Zhedong Zheng, Liang Zheng, Michael Garrett, Yi Yang, Mingliang Xu, and Yi-Dong Shen. 2020. Dual-path convolutional image-text embeddings with instance loss. *ACM Transactions on Multimedia Computing, Communications, and Applications (TOMM)* 16, 2 (2020), 1–23.
- [55] Aichun Zhu, Zijie Wang, Yifeng Li, Xili Wan, Jing Jin, Tian Wang, Fangqiang Hu, and Gang Hua. 2021. DSSL: Deep Surroundings-person Separation Learning for Text-based Person Retrieval. In *Proceedings of the 29th ACM International Conference on Multimedia*. 209–217.
- [56] Jialong Zuo, Hanyu Zhou, Ying Nie, Feng Zhang, Tianyu Guo, Nong Sang, Yunhe Wang, and Changxin Gao. 2023. UFBench: Towards Text-based Person Retrieval with Ultra-fine Granularity. arXiv:2312.03441 [cs.CV]

## A EXPERIMENTAL SETTINGS

### A.1 Datasets

We evaluate the proposed framework based on on three widely-used TBPS datasets: CUHK-PEDES [31], ICFG-PEDES [10] and RSTPReid [55], and a newly released dataset: UFBench [56].

**CUHK-PEDES** [31] is the first benchmark for TBPS, with 40, 206 images, 80, 440 texts, and 13, 003 identities. Each image has an average of two textual descriptions. Following the official data split, the training dataset contains 34, 054 images and 68, 126 texts from 11, 003 identities, the validation set consists of 3, 078 images and 6, 158 texts from 1, 000 identities, and the test set has 3, 074 images and 6, 156 texts from 1, 000 identities.

**ICFG-PEDES** [10] has 54, 522 images from 4, 102 identities. Each image has one textual description. The dataset is split into a training set with 34, 674 images from 3, 102 identities, and a test set with 19, 848 images from 1, 000 identities.

**RSTPReid** [55] consists of 20, 505 images of 4, 101 identities. Each identity has five images from different cameras, each with two textual descriptions. The training, validation, and test datasets have 3, 701, 200, and 200 identities, respectively.

**UFBench** [56] contains 26, 206 images and 52, 412 descriptions of 6, 926 persons totally. The textual annotations have ultra-fine granularity, with the average word count three to four times that of the previous datasets. The training and test set contains 4926 and 2, 000 identities respectively.

### A.2 Evaluation Metrics

We adopt the Rank-k (R-k for simplicity, k=1, 5, 10) as the evaluation metrics. These metrics assess the probability of locating at least one matching person image within the top-k candidates, given a text as the query. Also, we adopt the mean average precision (mAP) as a complementary metric, which measures the average retrieval performance in scenarios where multiple ground-truths exist.

### A.3 Implementation Details

We conduct all experiments on 4 NVIDIA A40 GPUs. For the generation model, we finetune it with a learning rate of  $1e-5$  and a batch size of 64 for 10 epochs, utilizing the Adam optimizer [26]. The retrieval model, on the other hand, is trained for 20 epochs with a learning rate of  $1e-5$  and a batch size of 64. We applied random horizontal flipping as a form of data augmentation for the image data. In the case of Hybrid Patch-channel Masking, we set the patch-level masking rates as  $\rho^v = 0.2$  and  $\rho^t = 0.1$ , respectively, the channel-level masking rates as  $\beta^v = 0.1$  and  $\beta^t = 0.1$ .

### A.4 Backbones

The proposed solution offers flexibility in selecting image captioning and text-based person retrieval backbones. Existing methods can be readily substituted as backbones. In our experiments, we employ multiple backbones, with BLIP being the default choice for generation and retrieval. The model architecture of BLIP has been discussed in the main paper.

**Table 7: Comparison with different variants of the proposed solution on CUHK-PEDES with 1% labeled data.**

Generation	Retrieval	R-1	R-5	R-10	mAP
<i>Using different generation models</i>					
<b>BLIP</b>	<b>BLIP</b>	<b>63.87</b>	<b>82.20</b>	<b>87.70</b>	<b>57.18</b>
BLIP-2	BLIP	62.12	80.96	87.18	56.57
<i>Using different retrieval models</i>					
<b>BLIP</b>	<b>BLIP</b>	<b>63.87</b>	<b>82.20</b>	<b>87.70</b>	<b>57.18</b>
BLIP	RaSa	61.96	80.69	86.87	55.29
BLIP	IRRA	56.17	76.49	83.85	50.99

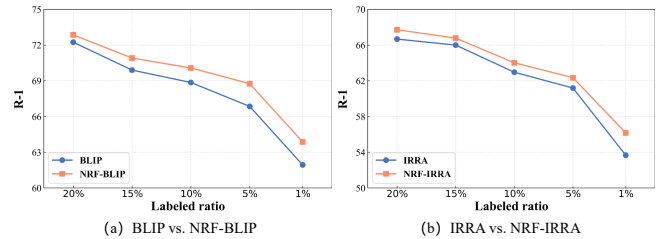
**Generation.** Apart from **BLIP**, the **BLIP-2** [28] is also utilized for image captioning. BLIP-2 is a versatile and highly efficient framework that leverages off-the-shelf frozen image encoders and large language models via a lightweight querying transformer. It enables effective vision-language pretraining and yields impressive results across various vision-language tasks, including image captioning. **Retrieval.** In addition to **BLIP**, we also conduct experiments on the recent popular TBPS methods **RaSa** [1] and **IRRA** [21]. RaSa leverages relation-aware learning and sensitivity-aware learning to mitigate the impact of weak cross-modal correspondence and facilitate representation learning in TBPS. IRRA introduces a cross-modal implicit relation reasoning module to enhance global image-text matching and a similarity distribution matching loss to amplify the correlations between matching pairs.

## B EXTENDED EXPERIMENTS

### B.1 Study on Scalability of Two-stage Solution

We propose a scalable solution for semi-supervised TBPS, in which the generation and retrieval models can be flexibly changed with existing methods. To verify the scalability of the proposed solution, in addition to the default backbone BLIP [29], we conduct a series of experiments with different model variants, including BLIP-2 [28] and BLIP-2 [28] for generation, RaSa [1] and IRRA [21] for retrieval. The experimental results are shown in Table 7.

**Generation.** From Table 7, we can observe that the proposed framework, whether utilizing BLIP or BLIP-2, consistently achieves excellent performance, thereby strongly validating its scalability. Furthermore, it is worth noting that the proposed framework with the default BLIP exhibits slightly stronger performance compared to using BLIP-2. We hypothesize that this discrepancy can be attributed to their distinct decoding strategies. BLIP employs nucleus sampling [18] as its decoding strategy, which is a stochastic method, while BLIP-2 utilizes the deterministic decoding method of beam search [12]. Due to its stochastic nature, nucleus sampling in BLIP tends to generate a greater diversity of pseudo-texts [29] when compared to beam search in BLIP-2. This diversity characteristic aligns well with the open-form nature of textual queries in TBPS, thereby benefiting the subsequent training of the retrieval model. **Retrieval.** From Table 7, we can clearly see that the proposed framework, whether using BLIP or RaSa, yields commendable results. In particular, the proposed framework with BLIP surpasses the performance of that with RaSa. We conjecture that it is because BLIP harvests stronger vision-language alignment capability than RaSa. We also observed that the proposed framework with IRRA achieves a relatively mediocre performance. This could potentially

**Figure 4: Study on effectiveness and generalizability of the proposed noise-robust retrieval framework (NRF) on CUHK-PEDES with decreasing ratios of labeled data.**

be attributed to IRRA’s higher sensitivity to misalignment and noise introduced by the pseudo-texts.

### B.2 Study on Effectiveness and Generalizability of Noise-robust Retrieval Framework

To comprehensively validate the effectiveness of the proposed noise-robust retrieval framework (NRF), we conduct experiments with default retrieval backbone BLIP [29] on CUHK-PEDES across different labeled ratios. Since the noise problem in pseudo texts is more severe with limited labeled data, we choose to experiment under a small labeled ratio 20% and further decrease it to 1% with an interval of 5% for exploration of learning with increasing noise. We denote BLIP equipped with NRF as NRF-BLIP. In addition, to verify the generalizability of NRF to other retrieval model, we extend IRRA [21] by NRF, denoted by NRF-IRRA. The experimental results are shown in Figure. 4, from which we can observe that: (1) NRF-BLIP consistently outperforms BLIP across all labeled ratios, which strongly verifies the effectiveness of our NRF in learning under the noisy circumstance. (2) NRF-IRRA is evidently superior to IRRA in all tests, which shows the generalizability of NRF. (3) With the decrease of labeled ratio, the noise problem in the pseudo-texts gets more severe, which poses more challenges on the subsequent learning of retrieval model. NRF brings more performance gains to the underlying retrieval model under smaller labeled ratios, which demonstrates the robustness of NRF.

### B.3 Study on the Labeled Ratio

To research the influence of the labeled ratio in the semi-supervised setting, we conduct experiments on CUHK-PEDES by varying the labeled ratio from 1% to 50% with an interval of 10%. We also provide the performance of the default backbone BLIP under the fully-supervised setting as the performance upper bound for reference, where 100% labeled data is used for training. The experimental results are shown in Fig. 5, from which we can observe that the performance of our framework gradually rises with the increasing amount of labeled data. When using only 20% labeled data, our framework can approach the fully-supervised counterpart with a relatively small gap. As the labeled ratio continues to increase, the growth rate of performance gets slower. We conjecture that this is possibly because the generation model has already learned most knowledge of person captioning with 20% labeled data. Further incorporating more labeled data may not increase the quality of generated pseudo-texts substantially. Thus, less performance gains would be obtained by the retrieval model trained subsequently.

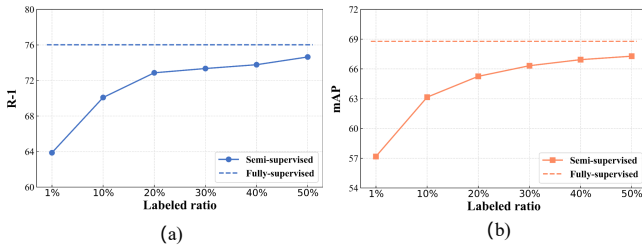


Figure 5: Study on the labeled ratio on CUHK-PEDES.

#### B.4 Parameter Analysis.

We introduce the Hybrid Patch-Channel Masking (PC-Mask) strategy to suppress the noise in the retrieval stage, where the parameter  $\rho^v$  and  $\rho^t$  is used to control the ratio of image and text patch-level masking,  $\beta^v$  and  $\beta^t$  is used to control the ratio of image and text channel-level masking, respectively. The influence of these parameters is shown in Fig. 6. (1) In terms of patch-level masking on both image and text, it can be observed that as  $\rho^v$  or  $\rho^t$  increase, Rank-1 and mAP initially rise and subsequently decline. The early-stage performance gain can be attributed to the increased efficacy of masking in separating noisy correspondences. However, as  $\rho^v$  continues to increase, valuable and essential semantic relations may be disrupted, impeding the model’s ability to learn cross-modal alignment and ultimately resulting in decreased performance. The peak Rank-1 performance is achieved at  $\rho^v = 0.2$  and  $\rho^t = 0.1$ , which are adopted in our experiments. (2) In terms of channel-level masking on both image and text, the Rank-1 and mAP also exhibit an initial increase followed by a subsequent decrease as the masking ratios increase. Notably, channel-level masking shows a more pronounced decline in performance compared to patch-level masking. The highest Rank-1 performance is achieved at  $\beta^v = 0.1$  and  $\beta^t = 0.1$ , which are the adopted ratios in our experiments.

#### B.5 Comparison with SoTAs on UFine6926

We compare the proposed framework with the state-of-the-art methods on a newly released dataset UFine6926 [56]. The textual annotations in UFine6926 show ultra-fine granularity, which poses a new challenge to the research of text-based person search. The experimental results are shown in Table 8. First, under the semi-supervised setting, our framework outperforms IRRA [21] and RaSa [1] consistently across all labeled ratios. In particular, when only 1% labeled data is available, the proposed framework surpasses IRRA and RaSa by 15% and 19.11% in terms of R-1, highlighting the advantages of the proposed framework. Second, when using 20% labeled data, our framework performs favorably against many SoTA methods from the fully-supervised setting. For example, our framework outperforms LGUR [40] and SSAN [10] by 10.29% and 5.89% at R-1, respectively. The promising performance on this ultra fine-grained dataset demonstrates the generalization ability and fitness of our framework towards the complex scenarios.

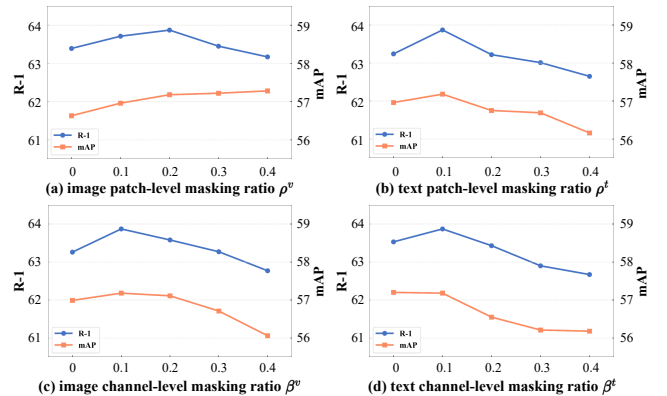


Figure 6: Retrieval performance under varying parameters of PC-Mask on CUHK-PEDES with 1% labeled data.

Table 8: Comparison with SOTA methods on UFine6926. “Labeled” refers to the amount of labeled training data.

Labeled	Methods	References	R-1	R-5	R-10	mAP
100%	NAFS [13]	Arxiv-2021	64.11	80.32	85.05	63.47
	LGUR [40]	ACMMM-2022	70.69	84.57	89.91	68.93
	SSAN [10]	Arxiv-2021	75.09	88.63	92.84	73.14
	IRRA [21]	CVPR-2023	83.53	92.94	95.95	82.79
	CFAM(B/16) [56]	CVPR-2024	85.55	94.51	97.02	84.23
20%	IRRA [21]	CVPR-2023	71.80	86.49	91.75	70.18
	RaSa [1]	IJCAI-2023	76.95	89.66	93.36	73.16
	Ours	-	80.98	92.25	95.29	79.40
5%	IRRA [21]	CVPR-2023	54.71	74.88	82.80	54.35
	RaSa [1]	IJCAI-2023	58.10	75.86	82.05	53.84
	Ours	-	75.60	88.75	92.83	74.06
1%	IRRA [21]	CVPR-2023	38.04	58.84	68.96	38.52
	RaSa [1]	IJCAI-2023	33.93	52.32	60.46	31.01
	Ours	-	53.04	71.24	78.98	52.58

## C VISUALIZATION ANALYSIS

**Visualization of Retrieval Results.** We exhibit three top-10 retrieval examples of the baseline and our framework trained with 1% labeled data in Fig. 7, where the first row and the second row in each example present the retrieval results from baseline and our framework, respectively. It can be seen that our framework can retrieve the corresponding pedestrian images for a query text more accurately. This is mainly due to the capability of our two-stage solution in exploiting both labeled and unlabeled data and the alleviation of noise interference by the powerful noise-robust retrieval framework. The visualization vividly demonstrates the effectiveness of our framework.

**More Examples of the Generated Pseudo-texts.** We provide more visualization results of human annotated texts and generated pseudo-texts from the vision-language model BLIP [29] under the zero-shot setting and finetuned on 1% labeled data in Fig. 8. We can see that pseudo-texts from zero-shot BLIP tend to be coarse-grained while those from finetuned BLIP possess more fine-grained details but may contain inevitable noise, as highlighted in red. Towards the noise problem in pseudo-texts, we propose the noise-robust retrieval framework to particularly address it.

**Query:** The woman has medium-brown hair to the middle of her back. She's wearing a white shirt, with sleeves to the elbow, and a light blue shirt. She has a blue purse across her shoulder.



Rank-1 → Rank-10

**Query:** The girl is wearing a white cap and her dark hair comes through the back of it. She is wearing a white t-shirt with red printed capris and light sandals. She is carrying a shopping bag.




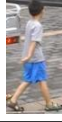

Rank-1 → Rank-10

**Query:** A male looking down at something in his hand. He has on a light grey shirt with long blue jean shorts. He has a black book bag on his back.



Rank-1 → Rank-10

**Figure 7: Visualization of top-10 retrieval results on CUHK-PEDES. The first row in each example presents the retrieval results from the baseline, and the second row shows the results from our framework. Correct/Incorrect images are marked by green/red rectangles.**

Image	BLIP zero-shot	BLIP finetuned	Human annotated
	Blurry image of woman in purple shirt with umbrella.	The man has short hair and glasses. He is wearing a bright purple shirt and khaki pants	The man has short medium brown hair and is wearing a short sleeve purple shirt with long medium brown shorts and dark brown shoes.
	A little boy wearing slippers walking across the street.	A woman wearing a short sleeve gray shirt with a blue skirt and brown shoes.	This person is visible from the side and is wearing a grey short sleeve tee shirt, bright blue shorts and sandals.
	Man walking down the street with bag of groceries on his back	the man is wearing black pants, a white shirt, and brown shoes he is also wearing dark colored short-sleeved boots	A man wearing a blue and white plaid shirt, a pair of black shorts and a pair of gray shoes.

**Figure 8: More visualization results of human annotated texts and generated pseudo-texts from the vision-language model BLIP [29] under the zero-shot setting and finetuned on 1% labeled data. Pseudo-texts from zero-shot BLIP tend to be coarse-grained while those from finetuned BLIP possess more fine-grained details but may contain inevitable noise. The noise is highlighted in red.**

## D LIMITATIONS

For the novel and resource-friendly semi-supervised TBPS, we develop a two-stage solution based on generation-then-retrieval. Based on it, our primary focus is on addressing the noise problem of pseudo-texts in the retrieval stage, leading to the proposal of a noise-robust retrieval framework. Furthermore, we acknowledge the importance of improving the performance of the generation model, as it can help mitigate the noise problem in the subsequent retrieval stage. However, this particular aspect remains unexplored in this paper. Particularly, current advanced generation models are pretrained vision-language models that exhibit exceptional performance in general domains. However, the effective adaptation of these pretrained vision-language models to the person-specific domain, given limited labeled data, poses an important challenge within our proposed two-stage solution. In the future, we will explore potential directions from the generation perspective. For instance, leveraging the robust few-shot learning capabilities of multimodal large language models could enable the generation of higher-quality pseudo-texts, thereby further facilitating the advancement of semi-supervised TBPS.